

AD-A037 149

BALLISTIC RESEARCH LABS ABERDEEN PROVING GROUND MD
NEGATIVE IONS IN CO₂. (U)

F/G 20/8

UNCLASSIFIED

FEB 77 T D FANSLER, L M COLONNA-ROMANO
BRL-1963

NL

| OF |

AD
A037149



					END		DATE FILMED		4 - 77				

AD A 037149

BKL K 1903

BRL

12
B.S.

AD

REPORT NO. 1963

NEGATIVE IONS IN CO₂

T. D. Fansler
L. M. Colonna-Romano
R. N. Varney

DDC
MAR 18 1977
C

February 1977

Approved for public release; distribution unlimited.

USA BALLISTIC RESEARCH LABORATORY
ABERDEEN PROVING GROUND, MARYLAND

Destroy this report when it is no longer needed.
Do not return it to the originator.

Secondary distribution of this report by originating
or sponsoring activity is prohibited.

Additional copies of this report may be obtained
from the National Technical Information Service,
U.S. Department of Commerce, Springfield, Virginia
22151.

The findings in this report are not to be construed as
an official Department of the Army position, unless
so designated by other authorized documents.

UNCLASSIFIED

SECURITY CLASSIFICATION OF THIS PAGE (When Data Entered)

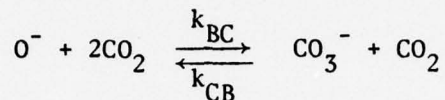
REPORT DOCUMENTATION PAGE		READ INSTRUCTIONS BEFORE COMPLETING FORM
1. REPORT NUMBER 14 BRL Report No. 1963	2. GOVT ACCESSION NO.	3. RECIPIENT'S CATALOG NUMBER
4. TITLE (and Subtitle) NEGATIVE IONS IN CO ₂	5. TYPE OF REPORT & PERIOD COVERED Final report	
7. AUTHOR(s) T. D. Fansler, L. M. Colonna-Romano and R. N. Varney*	6. PERFORMING ORG. REPORT NUMBER	
9. PERFORMING ORGANIZATION NAME AND ADDRESS US Army Ballistic Research Laboratory Aberdeen Proving Ground, Maryland 21005	8. CONTRACT OR GRANT NUMBER(s)	
11. CONTROLLING OFFICE NAME AND ADDRESS US Army Materiel Development & Readiness Command 5001 Eisenhower Avenue Alexandria, Virginia 22333	10. PROGRAM ELEMENT, PROJECT, TASK AREA & WORK UNIT NUMBERS RDTE: 1T161102B53A SA4 DNA Subtask S99QAXHD010	
14. MONITORING AGENCY NAME & ADDRESS (if different from Controlling Office)	12. REPORT DATE FEBRUARY 1977	13. NUMBER OF PAGES 33
	15. SECURITY CLASS. (of this report) Unclassified	
16. DISTRIBUTION STATEMENT (of this Report) Approved for public release; distribution unlimited.		
17. DISTRIBUTION STATEMENT (of the abstract entered in Block 20, if different from Report)		
18. SUPPLEMENTARY NOTES * NRC Senior Research Associate		
19. KEY WORDS (Continue on reverse side if necessary and identify by block number) Atmospheric Ions Ion-Molecule Reaction Negative Ion Clusters Electron Detachment Drift Tubes Reaction Rate Coefficient Negative Ion Chemistry		
20. ABSTRACT (Continue on reverse side if necessary and identify by block number) (enl) Reaction rate coefficients for negative ions in carbon dioxide have been investigated in a drift tube by analysis of time-of-arrival spectra. Collisional detachment of electrons, clustering of the negative atomic oxygen ion to carbon dioxide, collisional dissociation of the carbon trioxide ion, and electron dissociative attachment have been studied at low pressure and over an order of magnitude range of the ratio of electric field to neutral number density (E/N), starting slightly above thermal. Changes of gas temperature have been shown to act to shift the reaction equilibrium in the same sense that changes in E/N do.		

DDC
RECEIVED
MAR 18 1977
RESOLVED
C

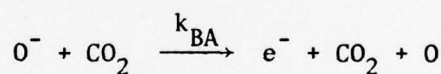
050 750

SUMMARY

Reaction rate coefficients for negative ions in CO_2 according to the reaction



have been evaluated experimentally over a range of $45 \leq E/N \leq 400$ Td at 320 ± 2 °K. Most of the measurements were made with a drift-tube mass-spectrometer operated in a mode to gate electrons as well as negative ions. The attachment of electrons in the drift tube introduces details into the arrival time spectra of the ions that enhance the resolving power for evaluation of rate coefficients. At low E/N , k_{BC} approaches $(5 \pm 0.5) \times 10^{-28} \text{ cm}^6 \text{ s}^{-1}$, and declines slowly with increasing E/N . The value of k_{CB} is negligible below $E/N = 300$ Td, then rises steeply to $\approx 1 \times 10^{-11} \text{ cm}^3 \text{ s}^{-1}$ at 400 Td. Changes of gas temperature have been shown to act to shift the reaction equilibrium in the same sense that changes in E/N do. At $E/N \geq 200$ Td, collisional detachment of electrons from O^- occurs according to the reaction



and the rate rises steeply with E/N . At 400 Td, k_{BA} reaches $9 \times 10^{-12} \text{ cm}^3 \text{ s}^{-1}$.

ACCESSION for	
NTIS	White Section <input checked="" type="checkbox"/>
DOC	Buff Section <input type="checkbox"/>
UNANNOUNCED	
JUSTIFICATION	
BY: _____	
DISTRIBUTION AVAILABILITY STATE	
Dist.	Avail. Section
A	

TABLE OF CONTENTS

	Page
SUMMARY.	3
LIST OF ILLUSTRATIONS.	7
I. INTRODUCTION	9
II. APPARATUS.	10
III. ION-ELECTRON-MOLECULE REACTIONS.	11
IV. EXPERIMENTAL OBSERVATIONS.	14
V. ANALYSIS OF ARRIVAL TIME SPECTRA	17
VI. VALUES OF RATE COEFFICIENTS.	18
VII. SOME ADDITIONAL DATA	21
VIII. TEMPERATURE STUDIES.	22
IX. PRECISION OF RATE COEFFICIENTS	25
X. CONCLUSIONS.	26
REFERENCES	27
DISTRIBUTION LIST.	29

PRECEDING PAGE BLANK NOT FILMED

LIST OF ILLUSTRATIONS

Figure	Page
1. Rate coefficient k_{BA} for collisional detachment of electrons from O^- . The left curve is for collisions of O^- with O_2 from Ref. (8). The right curve shows present findings for O^- collisions with CO_2	13
2. A typical set of arrival time spectra for O^- ions in CO_2 at $E/N = 200$ Td and at three different pressures. All three curves were obtained with gating conditions that pulsed electrons as well as negative ions. The gated electrons continue to attach throughout the drift distance, and ion-molecule reactions also occur. Ordinates are normalized for equal areas under curves. Channels are 2 μs wide. No correction for analysis time has been included.	15
3. A typical set of arrival time spectra for CO_3^- ions in CO_2 at $E/N = 650$ Td and at two different pressures. The high value of E/N was chosen to display the results when dissociation of CO_3^- , detachment of O^- , and Townsend electron multiplication are all occurring. Normalized as in Fig. 3. Channel width is 1 μs . No correction for analysis time has been included.	16
4. Display of the match achieved by computed arrival time spectra with experimental spectra. Upper illustration shows the comparison for O^- , lower illustration for CO_3^- , at the same E/N and p . Channel width is 2 μs . No correction for analysis time has been included. Solid curves are computed; points are experimental results.	19
5. Experimental findings for rate coefficients k_{BC} and k_{CB} , the formation and dissociation of CO_3^- , respectively. Data of Moseley, Cosby, and Peterson (MCP), ref. (16), are also shown. Open circles represent results from analysis of arrival time spectra. Solid circles represent results from analysis of ion currents (dc) as a function of drift distance.	20
6. Graphs of the non-gated current ratio of CO_3^- ions to total ion current as a function of E/N at three different gas temperatures. The curves are used to correlate changes in gas temperature with equivalent changes in E/N	23

PRECEDING PAGE BLANK - NOT FILMED

I. INTRODUCTION

In this paper, we report our study of negative ions in CO_2 at various temperatures, pressures, and values of E/N (the ratio of electric field strength to molecular density) ranging from 45 to 400 Td ($1 \text{ Td} = 10^{-17} \text{ V cm}^2$). The study includes findings concerning identity of the system of negative ions and the various reaction rates for their formation and breakup. The results were made possible by the application of an experimental technique that adds great resolving power to the determination of the coefficients. Basically, the experimental procedure consists of the use of a drift-tube mass-spectrometer, equipped for measurement of the arrival time spectra of the negative ions.⁽¹⁾⁽²⁾ Its novel feature is that the electrons that unavoidably accompany negative ions from the source are also gated by the Tyndall shutter that gates the negative ions. This procedure has been used earlier by Pack and Phelps⁽³⁾ on negative ions in O_2 in a variant form of the present usage. Experimentally, a much higher gate bias voltage is needed in order to pulse the electron stream than is necessary for negative ions alone as the electrons have a much higher kinetic energy than the ions. Bias voltages as high as 22.5 V have been used, and correspondingly, a high pulse voltage to open the gate. The electrons admitted during the gate pulses continue to attach to form negative ions in the drift space. The resulting arrival time spectra are intricate but are far richer in information than those obtained with the more usual gate bias that only pulses the negative ions. As has been noted, both by us and by others,⁽⁴⁾ with the low-voltage gate bias, there is a continuous background of electron current through the drift tube that causes variations with pressure in rate coefficients which should in principle be constant. We note that, in

¹G. E. Keller, R. A. Beyer, and L. M. Colonna-Romano, Phys. Rev. A 8, 1446 (1973).

²I. R. Gatland, L. M. Colonna-Romano, and G. E. Keller, Phys. Rev. A 12, 1885 (1975).

³J. L. Pack and A. V. Phelps, J. Chem. Phys. 44, 1870 (1966).

⁴H. W. Ellis, R. Y. Pai, I. R. Gatland, E. W. McDaniel, R. Wernlund, and M. J. Cohen, J. Chem. Phys. 64, 3935 (1976).

addition, the arrival time spectra with the low gate bias are only slightly perturbed from the simple skewed-Gaussian shape characterizing pure diffusion (in marked contrast to our present spectra), giving poorer resolution for even the principal rate coefficients.

II. APPARATUS

The apparatus has been described in other publications⁽¹⁾⁽²⁾ and is accordingly only briefly reviewed here; the electron-impact ion source is the only significant change. A hot cathode coated with BaZrO_3 ⁽⁵⁾ emits electrons which are then accelerated by suitable electrodes in a direction transverse to the main axis of the drift-tube mass-spectrometer. There is also a magnetic field of strength about 100 G in the same direction, provided by a permanent magnet. The acceleration potential is typically about 9 V, at which the attachment of electrons in CO_2 is near its maximum value.⁽⁶⁾ The electrons cross the axis of the drift tube, and the surplus are collected in a Faraday cage. Between the electron gun and the Faraday cage, the electrons pass between a repeller plate and a parallel grid. Some of the negative ions formed by attachment of electrons to gas molecules in this space are repelled by the plate and pass through the grid where they enter the first stages of the drift tube. Some electrons also escape into the drift space despite the magnetic field. Two additional grids beyond the extracting grid form a 2.7-cm long thermalizing region, usually (but not always) having the same electric field as the main drift region. Gas, CO_2 in the present work, fills both the source and the drift tube to the desired pressure, ranging in this work from 13.3 to 66.7 Pa (0.10 to 0.50 torr).

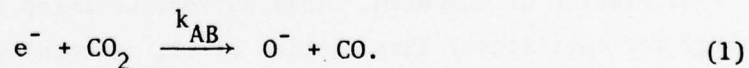
⁵D. MacNair, *Rev. Sci. Instrum.* 38, 124 (1967).

⁶G. L. Schulz, *Phys. Rev.* 128, 178 (1962). See also, E. W. McDaniel, *Collision Phenomena in Ionized Gases* (John Wiley & Sons, Inc. New York, 1964) p. 419.

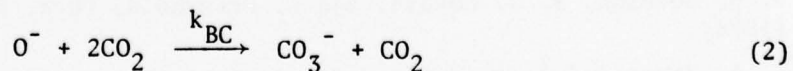
The main drift space has two Tyndall shutters, one of which is electrically biased to inhibit the drift of ions and/or electrons. To gate the electrons, we have usually used 22.5 V bias across the 3.2-mm shutter grids. With the source operating continuously, the biased gate is pulsed to allow a small group of ions and electrons to drift down the tube. A sampling aperture (0.4 mm diameter) terminates the drift region, which was of length 6.45 cm for most of the work reported here. From the exit aperture, the ions (and electrons) pass through a differentially pumped chamber into a monopole mass spectrometer where the individual ions are detected. The only ionic species present in appreciable quantity are atomic masses 16 (O^-) and 60 (CO_3^-). Electrons cannot be detected with the present equipment. Base pressure after baking of the ion source and drift region is 7×10^{-7} Pa (5×10^{-9} torr). The arrival time spectra were all obtained at a temperature of 320 ± 2 °K.

III. ION-ELECTRON-MOLECULE REACTIONS

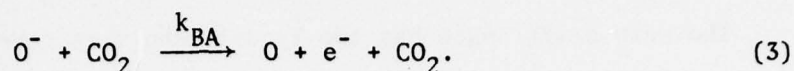
The analysis of reactions is made by use of preliminary qualitative knowledge of what reactions occur, followed by the experimental verification of the reactions and the determination of their rate coefficients. The negatively charged particles involved are electrons, O^- ions, and CO_3^- ions, whose currents are designated A, B, and C respectively when such brevity is necessary. In the source as well as in the drift tube, the electrons attach by dissociative attachment shown by the reaction



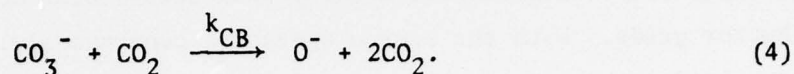
The quantity k_{AB} is the reaction rate coefficient, the subscripts designating that A (e^-) changes to B (O^-). O^- ions may be lost by the clustering reaction:



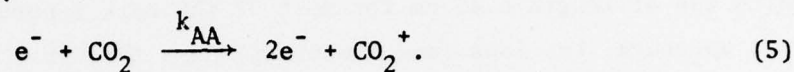
with the three-body reaction rate coefficient k_{BC} , and, at higher values of E/N, by collisional detachment:



At still higher E/N, the reverse of reaction (2) can occur endothermically:



Finally, at sufficiently high E/N, the Townsend process of electron multiplication can occur:



The CO_2^+ drifts away from the mass spectrometer and is not detected.

Reactions (1) - (5) form a complex system, particularly at high E/N where all five processes may contribute significantly. Reaction (1) has been studied previously.⁽⁷⁾ The attachment coefficient η , obtained from Ref. (7), is used to calculate the reaction rate coefficient k_{AB} by the equation $k_{\text{AB}} = \frac{\eta}{N} v_D$, where v_D is the electron drift velocity and N is the neutral number density. Some information bearing on reaction (3) is available from the analogous process of detachment of electrons from O^- in collision with O_2 which has been measured by Goodson, Corbin, and Frommhold;⁽⁸⁾ their values of k_{BA} at various E/N are shown in Fig. 1.

The photodissociation of CO_3^- into O^- and CO_2 has been measured to set in at photon energies of 1.8 ± 0.1 eV,⁽⁹⁾⁽¹⁰⁾ a value applicable to reaction (4) subject to the usual corrections for the requirements of conservation of momentum. This correction makes the minimum kinetic energy for collisional dissociation of CO_3^- according to reaction (4)

⁷J. Dutton, "A Survey of Electron Swarm Data," J. Phys. Chem. Ref. Data, 4, 681 (1975).

⁸D. W. Goodson, R. J. Corbin, and L. Frommhold, Phys. Rev. A 9, 2049 (1974).

⁹R. A. Beyer and J. A. Vanderhoff, J. Chem. Phys. 65, 2313 (1976).

¹⁰J. T. Moseley, P. C. Cosby, R. A. Bennett, and J. R. Peterson, J. Chem. Phys. 65, 2512 (1976).

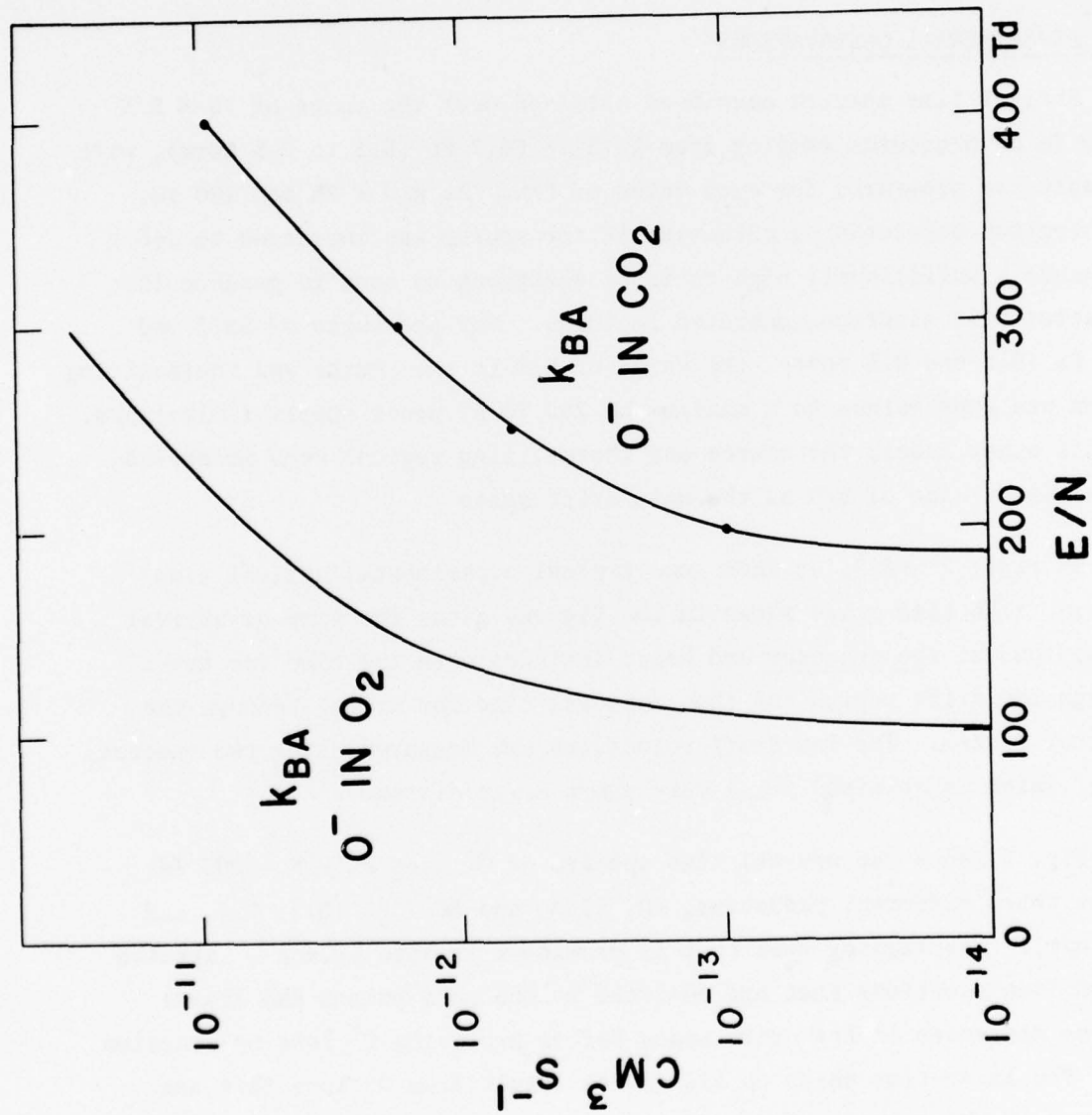


Figure 1. Rate coefficient k_{BA} for collisional detachment of electrons from O^- . The left curve is for collisions of O^- with O_2 from Ref. (8). The right curve shows present findings for O^- collisions with CO_2 .

become 4.35 eV. So large a value suggests that k_{CB} can only take on an experimentally significant value at high E/N. These various pieces of information provide useful guidelines for the procedures to be described.

IV. EXPERIMENTAL OBSERVATIONS

Arrival time spectra have been obtained over the range of $75 \leq E/N \leq 400$ Td at pressures ranging from 13.3 to 66.7 Pa (0.1 to 0.5 torr), with at least two pressures for each value of E/N. At E/N = 75 and 100 Td, the electron accelerating potential in the source was increased to 165 V to insure a sufficiently high ratio of electrons to ions to produce the characteristic electron-generated features. For pressures of 53.3 and 66.7 Pa (0.4 and 0.5 torr), the value of E/N in the source and thermalizing region was constrained to a maximum of 200 Td by power supply limitations. For all other cases, the source and thermalizing regions were maintained at the same value of E/N as the main drift space.

In Figs. 2 and 3, we show some typical experimental arrival time spectra. The time scale shown in the figures gives the time of arrival of the ions at the detector and hence includes both the time for travel through the drift region and the (unknown) time for travel through the detector system. The ion drift velocities are measured using two spectra, one of which is obtained for a very short drift distance. ⁽¹⁾⁽²⁾

Fig. 2 shows the arrival time spectra of O^- ions at E/N = 200 Td and at three different pressures, 40, 53.3, and 66.7 Pa (0.3, 0.4, and 0.5 torr). The leading foot that is prominent in some of the O^- spectra arises from electrons that are admitted by the gate pulses and travel various distances in the drift space before producing O^- ions by reaction (1). The later-time peaks on all curves result from O^- ions that are produced in the source and are admitted in pulses by the gate. The absence of any trailing foot on the O^- spectral curves of Fig. 2 indicates that the dissociation of CO_3^- into O^- by reaction (4) is negligible in this range of E/N. Note that although the fractional loss of electrons

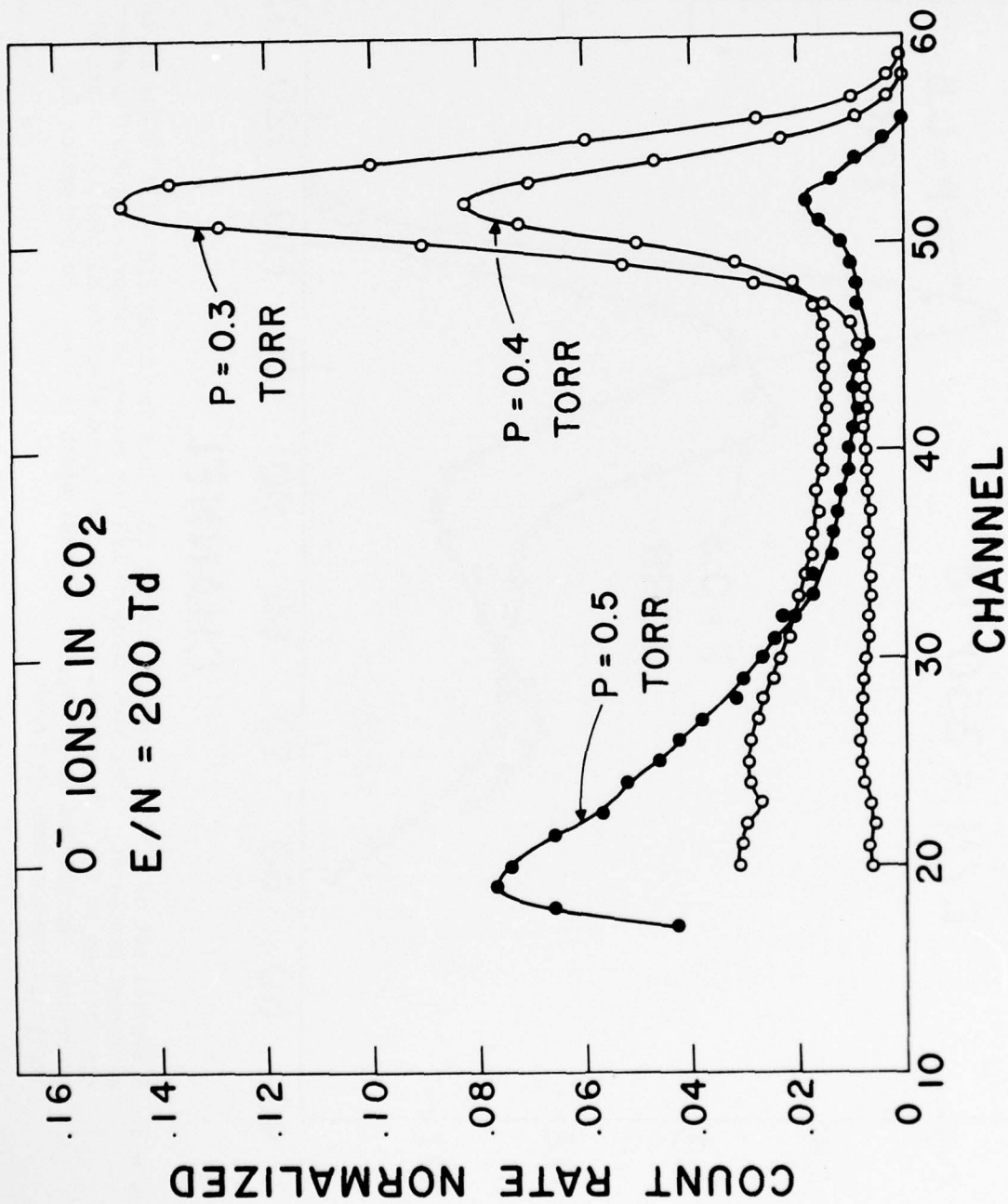


Figure 2. A typical set of arrival time spectra for O^- ions in CO_2 at $E/N = 200$ Td and at three different pressures. All three curves were obtained with gating conditions that pulsed electrons as well as negative ions. The gated electrons continue to attach throughout the drift distance, and ion-molecule reactions also occur. Ordinates are normalized for equal areas under curves. Channels are $2 \mu s$ wide. No correction for analysis time has been included.

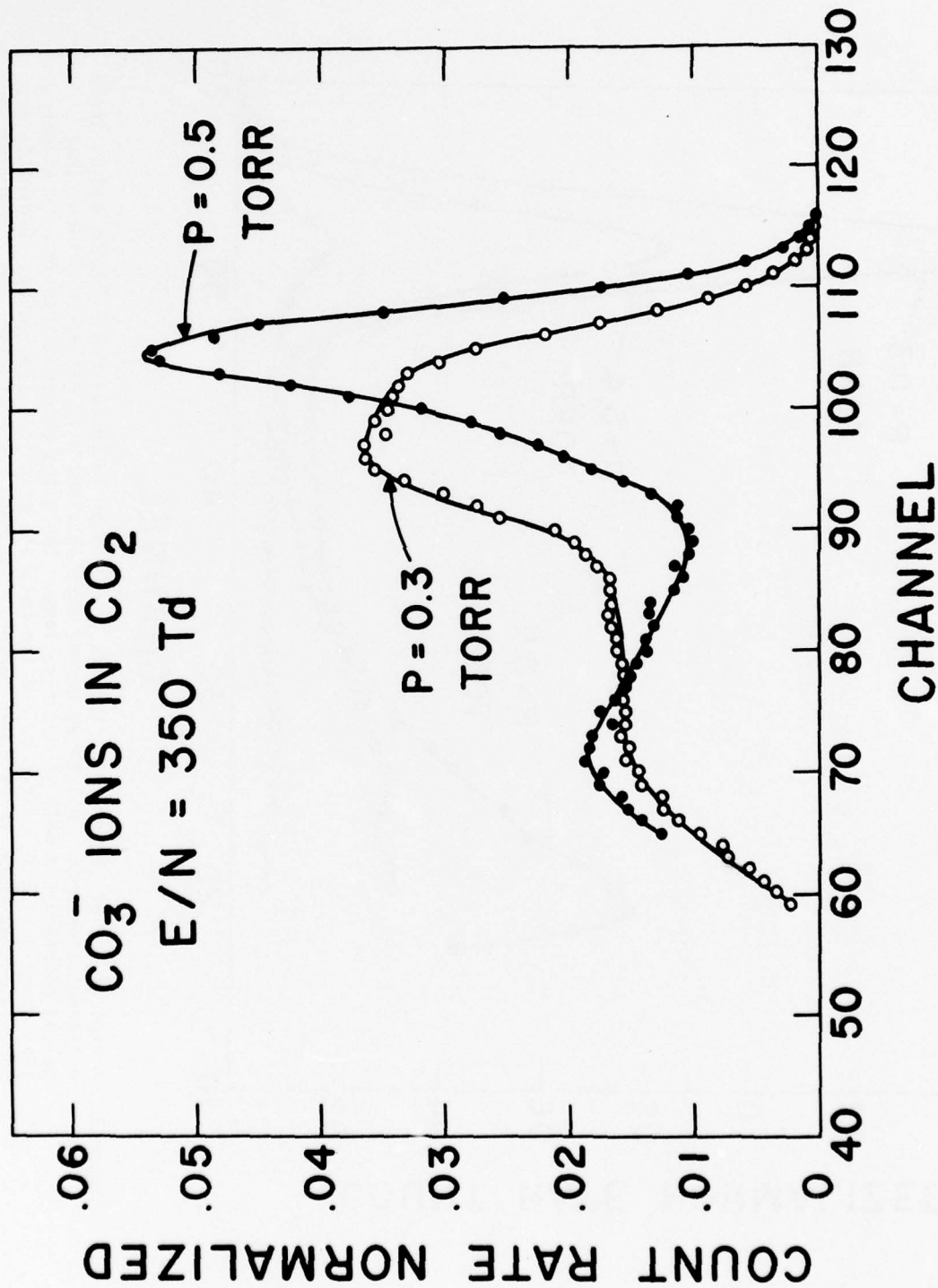


Figure 3. A typical set of arrival time spectra for CO_3^- ions in CO_2 at $E/N = 350 \text{ Td}$ and at two different pressures. The high value of E/N was chosen to display the results when dissociation of CO_3^- , detachment of O^- , and Townsend electron multiplication are all occurring. Normalized as in Fig. 3. Channel width is $1 \mu\text{s}$. No correction for analysis time has been included.

due to attachment during flight through the drift region is only a few per cent, the resulting number of O^- ions is comparable to (and often considerably exceeds) the number of O^- ions that are produced in the source and survive transit through the drift tube.

Fig. 3 shows two arrival time spectra for CO_3^- ions at $E/N = 350$ Td and $p = 40$ and 66.7 Pa (0.3 and 0.5 torr). Although these and other spectra have a decidedly intricate form, they offer by the same token a high degree of discrimination in the determination of the various rate coefficients.

V. ANALYSIS OF ARRIVAL TIME SPECTRA

Rate coefficients for reactions (2), (3), and (4) have been extracted from the experimental data by the method of Kregel *et al.*⁽¹¹⁾ Numerical integration of the differential equations describing the simultaneous chemical reaction, drift, and diffusion (both longitudinal and transverse) of the electrons and ions in the drift tube yields a predicted arrival time spectrum which is compared with the experimental data. As input for this calculation, we take the reaction rate coefficients for electron attachment, k_{AB} , and Townsend electron multiplication, k_{AA} , from the literature,⁽⁷⁾⁽¹²⁾ as well as the electron drift velocities and diffusion coefficients.⁽¹³⁾ Drift velocities of O^- and CO_3^- are measured in the experiment and the ion diffusion coefficients are computed from the experimental drift velocities via the Wannier formula.⁽¹⁴⁾

¹¹M. D. Kregel, M. R. Sullivan, L. M. Colonna-Romano, and G. E. Keller, NAPS Document #02183; order from ASIS/NAPS c/o Microfiche Publications, 305 E. 46 St., New York, N.Y. 10017. See also Ballistic Research Labs. Report No. 1617 (AD 907581).

¹²J. Dutton, *op. cit.*, p. 720.

¹³*Ibid.*, p. 605, 662-663.

¹⁴G. H. Wannier, *Phys. Rev.* **83**, 281 (1951); **87**, 795 (1952). See also E. W. McDaniel and J. T. Moseley, *Phys. Rev. A* **3**, 1040 (1971) or E. W. McDaniel and E. A. Mason, *The Mobility and Diffusion of Ions in Gases*, (John Wiley & Sons, Inc., New York, 1973) p. 314.

The theoretical spectra are then fit to the data by treating as variable parameters the initial electron and ion currents and the reaction rates for CO_3^- formation (k_{BC}), CO_3^- dissociation (k_{CB}), and electron detachment from O^- (k_{BA}). At a given value of E/N , we fit the data for two or more pressures simultaneously with one set of rate coefficients, allowing only the initial electron and ion currents to vary between these pressures. A comparison of the experimental data with the best-fit calculation is shown in Fig. 4 for the case of $E/N = 200$ Td and $p = 53.3$ Pa (0.4 Torr).

Experience has enabled us to recognize how changes in the rate coefficients alter the predicted arrival time spectra. Thus, the negative slope of the leading foot in the O^- spectra reflects the loss processes for O^- , reactions (2) and (3); whereas the positive slope of the leading portion in most of the CO_3^- spectra is due solely to conversion of O^- to CO_3^- via reaction (2). Reactions (2) and (3) are further distinguished by their different pressure dependence. The onset of collisional dissociation of CO_3^- , reaction (4), is indicated by the presence of a late-time tail on the source-generated O^- peak. Finally, we have found that Townsend electron multiplication, reaction (5), must be included to obtain a satisfactory fit of the early peak in the CO_3^- spectrum at, e.g., $E/N = 350$ Td and $p = 66.7$ Pa (0.5 torr) in Fig. 3.

VI. VALUES OF RATE COEFFICIENTS

In Fig. 5, we present the values of the attachment coefficient k_{BC} and the dissociation coefficient k_{CB} as functions of E/N . Since these two coefficients are the rates for the same reaction in the forward and backward directions, they are plotted in the same figure despite the need for separate ordinate scales. The ratio of the rate coefficients gives the equilibrium constant for the reaction. At $E/N = 400$ Td and $p = 66.7$ Pa (0.5 torr), the arrival time spectra reveal that the O^- and CO_3^- ions are nearly in equilibrium after drifting the length of the tube.

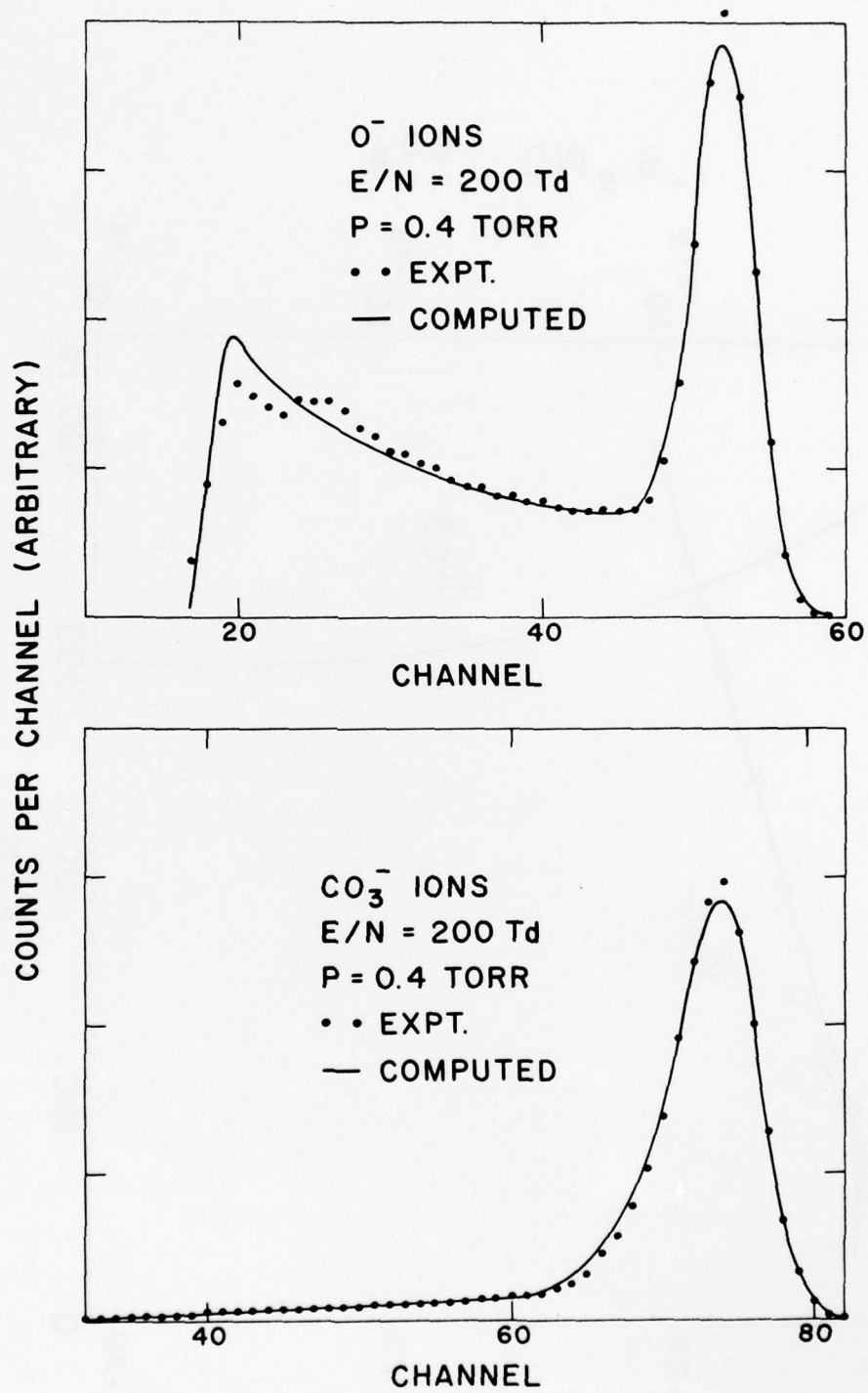


Figure 4. Display of the match achieved by computed arrival time spectra with experimental spectra. Upper illustration shows the comparison for O^- , lower illustration for CO_3^- , at the same E/N and p . Channel width is $2 \mu s$. No correction for analysis time has been included. Solid curves are computed; points are experimental results.

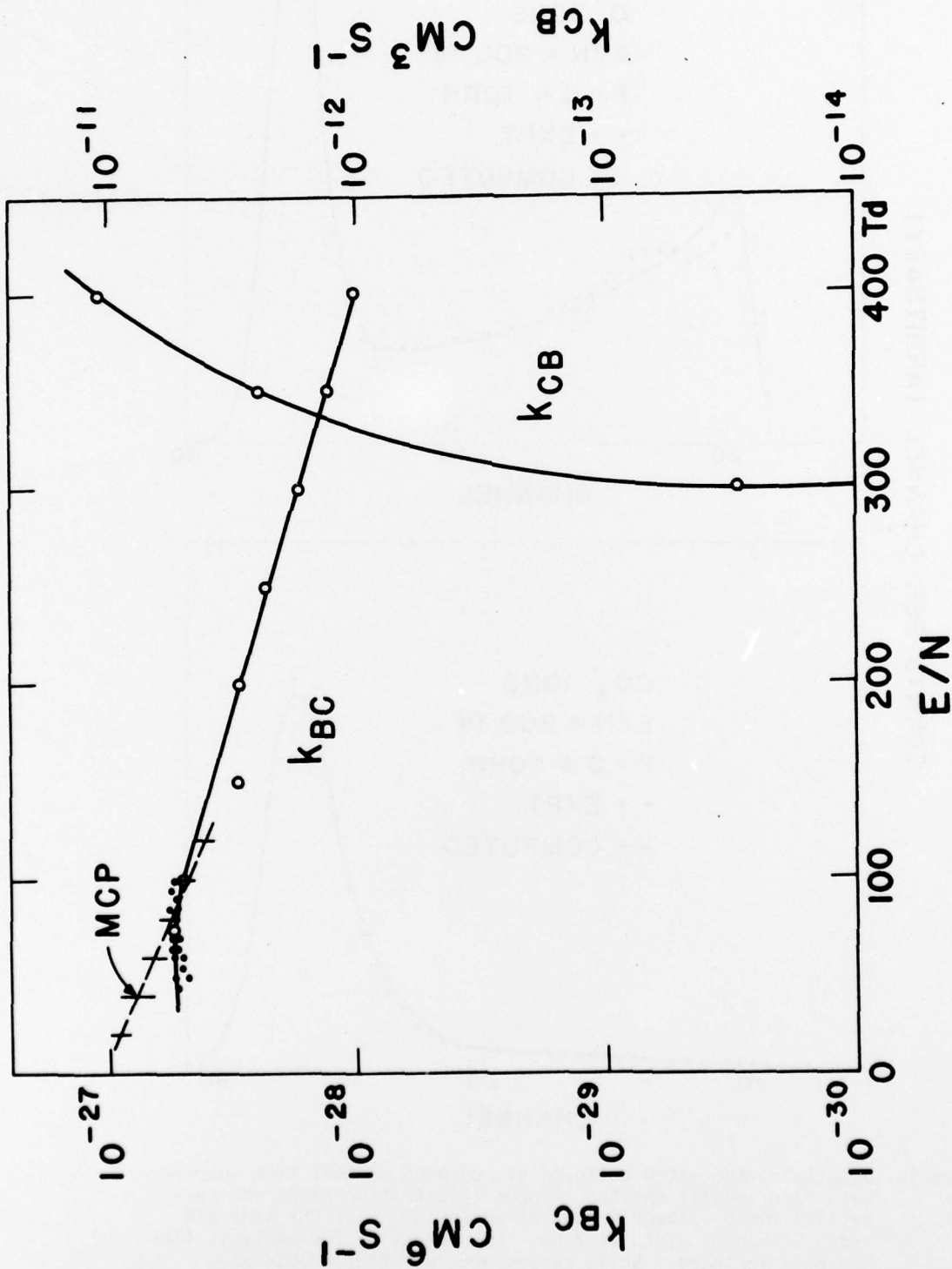


Figure 5. Experimental findings for rate coefficients k_{BC} and k_{CB} , the formation and dissociation of CO_3 , respectively. Data of Moseley, Cosby, and Peterson (MCP), ref. (16), are also shown. Open circles represent results from analysis of arrival time spectra. Solid circles represent results from analysis of ion currents (dc) as a function of drift distance.

Returning to Fig. 2 where k_{BA} is plotted from the results of Goodson, *et al.*⁽⁸⁾ for collisional detachment of O^- in O_2 , we have added our data for the same detachment in collisions with CO_2 . It has been suggested⁽¹⁵⁾ that the observed shift to higher E/N of the O^- electron detachment reaction rate in CO_2 is due to the lower O^- center-of-mass kinetic energy. Indeed, we have found that if the abscissa of Fig. 2 is changed to the center-of-mass kinetic energy, the two curves very nearly coincide.

Finally, we note that values of k_{AB} are not determined by this work as the quantity only appears multiplied by the electron current, which is not measured.

VII. SOME ADDITIONAL DATA

An alternative method for reaction rate studies of the present ion-molecule reactions consists of setting both Tyndall shutters open and observing comparative arrival currents of O^- and CO_3^- ions at the multiplier with several different lengths of the drift space. If two different drift distances are used, the change in the ratio $B/(B + C)$, (O^- current to total ion current) discloses the extent of reaction that has occurred with the increase in drift length. Analytically, it is clear that for each additional drift distance used, an additional unknown reaction rate coefficient can be evaluated. Operationally, the presence of an unknown and non-constant background current of electrons makes the method somewhat impractical. In the present work, we used four drift distances (3.76, 5.64, 7.52, and 9.40 cm); we confine our reported results by this method to values of E/N in the range between 45 and 120 Td and pressures of 13.3 and 26.6 Pa (0.10 and 0.20 torr). In this range, the only significant rate coefficient is k_{BC} , but the existence of the electron flux alters the O^- current at various drift distances through the rate coefficient k_{AB} and reaction (1). The values of k_{AA} , k_{BA} , and k_{CB} are quite

¹⁵We are indebted to Dr. R. J. Corbin for this suggestion.

negligible in this range. The values of k_{BC} obtained by this method shifted from $6 \times 10^{-28} \text{ cm}^6 \text{ s}^{-1}$ at $p = 0.1$ torr to 3×10^{-28} at 0.2 torr, a shift that could be attributed to the background current of electrons. At a fixed pressure, the value of k_{BC} remained constant over the whole range of E/N used, 45 to 120 Td. The points shown in Fig. 6 are adjusted to match the arrival time results at 75 and 100 Td. The findings of Moseley, Cosby, and Peterson⁽¹⁶⁾ are also shown in Fig. 5.

VIII. TEMPERATURE STUDIES

Following the dc procedure of Section VII, the ratio

$$Q = C/(B + C)$$

was measured at fixed p , z , and T (z is the drift distance) at a range of values of E/N from 50 to 300 Td. As might be expected, the value of Q started at nearly unity at $E/N = 50$ Td and decreased with increasing E/N . The gas temperature was then increased by 33°K by warming the entire tube, and the readings were repeated. Finally, one more temperature increase of 33° was made and Q vs. E/N again noted. A typical set of results is shown in Fig. 6. With each increase in temperature, the curve of Q vs. E/N is displaced horizontally toward lower E/N . A given value of Q is thus obtained at lower E/N the higher the gas temperature is made. A functional relation between E/N and T_g (the gas temperature) can be found from these results by choosing a value of Q and plotting T_g as ordinate against E/N as abscissa. To the very limited precision of the results, the points for any Q fall on a line, and by very long extrapolation to $E/N = 0$, a scale for converting E/N to an equivalent or effective temperature T_{eff} can be found. After numerous repetitions, a relationship

$$T_{\text{eff}} = T_g + 2.36 (E/N) \quad (6)$$

with E/N in Td and the temperatures in $^\circ\text{K}$ has been found. Such a procedure was first used by Varney⁽¹⁷⁾ on N_4^+ and N_2^+ ions in N_2 . We refrain from

¹⁶J. T. Moseley, P. C. Cosby, and J. R. Peterson, J. Chem. Phys. 64, 4228 (1976).

¹⁷R. N. Varney, Phys. Rev. 174, 165 (1958); J. Chem. Phys. 31, 1314 (1959).

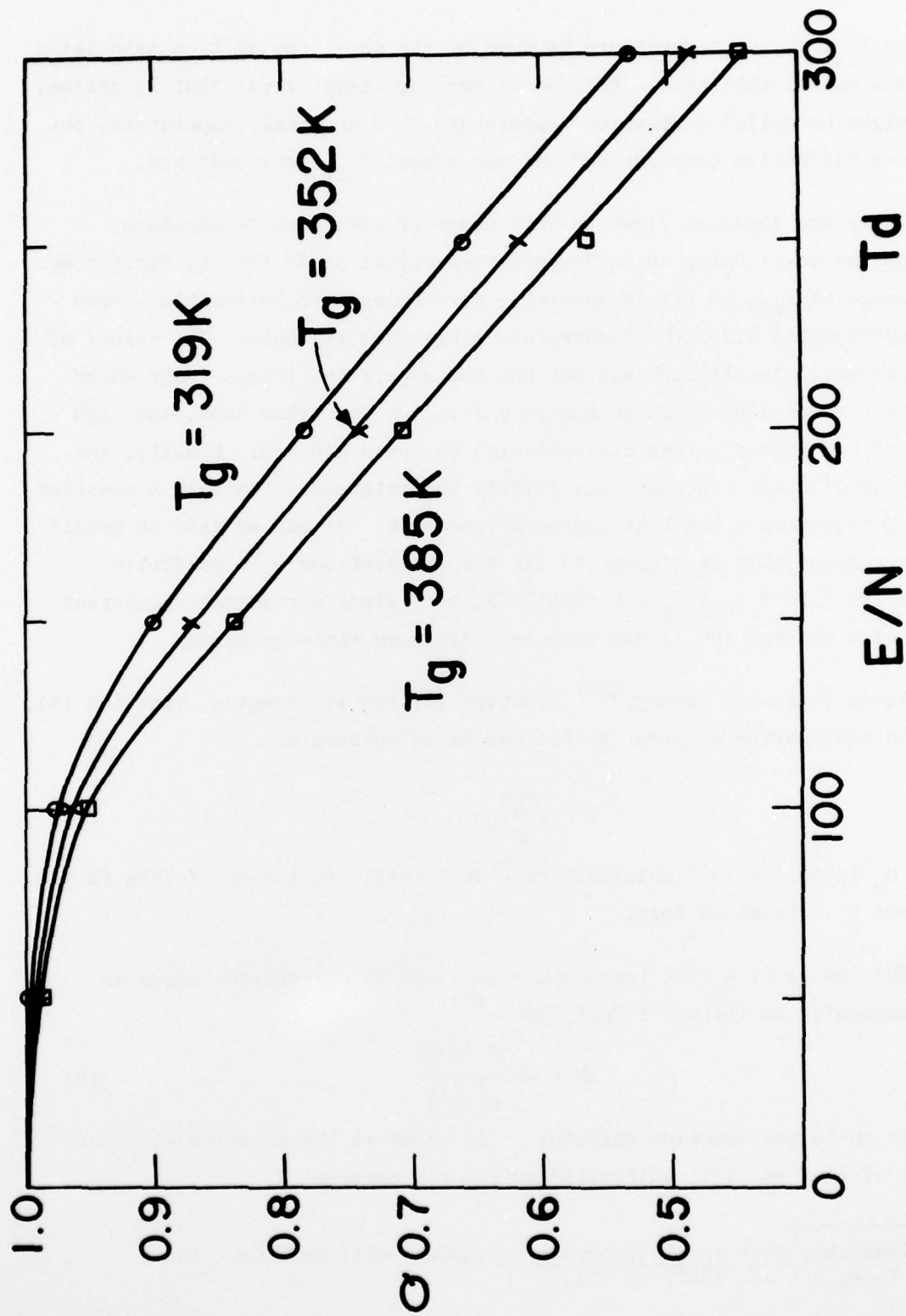


Figure 6. Graphs of the non-gated current ratio of CO_3^- ions to total ion current as a function of E/N at three different gas temperatures. The curves are used to correlate changes in gas temperature with equivalent changes in E/N .

calling T_{eff} an ion temperature because of the many complexities associated with the use of that term. Because of the experimental way that it arises, T_{eff} might be called a reaction temperature or a chemical temperature, but the name "effective temperature" and the symbol T_{eff} seem suitable.

There are apparent flaws in this usage of effective temperature, perhaps the worst being an inadequate theoretical basis for the first power dependence of T_{eff} on E/N , a quadratic form being more believable. From the experimental side, the temperature range used is small. The values of E/N , however, are all high and may put the experiment into a range where the first power dependence on E/N is valid. On the other hand, the high range of E/N forces a long extrapolation to reach $E/N = 0$. Finally, the interplay of other reactions may falsify the interpretation that a constant ratio Q signifies a constant degree of reaction. It may be said on behalf of the concept that an attempt to fit the observations by a quadratic law of the form $T_{\text{eff}} = T_g + b (E/N)^2$ fails to yield a reasonably constant value of b whereas the linear form does fit more satisfactorily.

Again following Varney,⁽¹⁷⁾ reaction (2) and its reverse, reaction (4), have an equilibrium constant \underline{K} that may be calculated as

$$\underline{K} = \frac{k_{\text{CB}}}{k_{\text{BC}} \cdot N_0} \quad (7)$$

where N_0 is 3.54×10^{16} molecules cm^{-3} at 1 torr. Inclusion of this factor N_0 gives \underline{K} in terms of torr.

The change of \underline{K} with temperature is given by an equation known in thermodynamics as the van't Hoff isobar⁽¹⁸⁾

$$\Delta H = -R \frac{d \ln \underline{K}}{d \left(\frac{1}{T} \right)} \quad (8)$$

wherein ΔH is the reaction enthalpy. Its value is the negative slope of a plot of $\ln \underline{K}$ vs. $1/T$, multiplied by the gas constant R .

¹⁸M. Zemansky, Heat and Thermodynamics (McGraw Hill Book Co., Inc. New York, 4th ed. 1957) p. 433.

In the case of ion-molecule reactions in the presence of an electric field, it is clear that T_g alone cannot be the correct temperature to use in the van't Hoff isobar, and the use of T_{eff} instead is indicated by the basic chemical nature in which T_{eff} arises. We have calculated $\ln K$ as $\ln(k_{\text{CB}}/k_{\text{BC}} \cdot N_0)$ at E/N of 350 and 400 Td and $1/T_{\text{eff}}$ using eq. (6). The resulting value of ΔH changes considerably with small changes in k_{CB} so that about all that can be said is that $\Delta H = 1.8 \pm 0.5$ eV. The value straddles that of refs. (9) and (10). Perhaps the most important aspect is the experimental observation that an equivalence exists between changes of E/N and changes of gas temperature.

IX. PRECISION OF RATE COEFFICIENTS

The precision of the evaluation of any given rate coefficient varies with the value of E/N. At E/N < 200 Td, the matching of computed with experimental curves is strongly influenced by small changes in k_{BC} because reaction (2) is the only one that plays any significant role and depends quadratically (hence strongly) on the gas pressure. A change in k_{BC} of $\pm 0.5 \times 10^{-28} \text{ cm}^6 \text{ s}^{-1}$ from the best-fit value clearly causes a mismatch of the curves. At higher E/N, where all the rate coefficients actively influence the various ion currents, several factors arise to diminish the precision, although the interactions still combine to give almost unique results. The greatest statistical spread arises for k_{BA} and k_{CB} , both of which change very steeply with E/N (see Figs. 1 and 5). At E/N = 350 Td, a change of $\pm 1 \times 10^{-12} \text{ cm}^3 \text{ s}^{-1}$ is barely detectable in mismatches between computed and experimental curves. Also, the combination of k_{AA} , k_{BA} , and k_{CB} , all of which enter combined with first-order pressure factors, can mutually compensate one another over a small range so that a variation of $\pm 1.5 \times 10^{-12} \text{ cm}^3 \text{ s}^{-1}$ is possible. The role of k_{BC} is less dominant in this range of E/N so that the precision of its determination would appear to be less, but a change of $\pm 0.5 \times 10^{-28} \text{ cm}^6 \text{ s}^{-1}$ still seems detectable.

X. CONCLUSIONS

The values of both k_{BC} and k_{CB} have been determined for a considerable range of values of E/N . The value of k_{CB} is negligible below $E/N = 300$ Td but rises steeply with E/N above this value. By contrast, k_{BC} varies only by about a factor of 5 from E/N of 50 to 400 Td. At low E/N , the value of k_{BC} is near to $5 \times 10^{-28} \text{ cm}^6 \text{ s}^{-1}$, a high value for a three-body rate coefficient. The reproducibility appears to lie well within $\pm 0.5 \times 10^{-28} \text{ cm}^6 \text{ s}^{-1}$.

The findings have been made possible by a new experimental procedure in which the drift tube gates are operated to gate electrons as well as negative ions. The technique greatly expands the information derivable from the arrival time spectra.

Rate coefficients k_{BA} for detachments of electrons from O^- in collisions with CO_2 have also been found as a function of E/N . The values of k_{BA} become negligible below E/N of 150 Td. The curve lies at higher E/N than that obtained for O^- detachment in O_2 obtained by Goodson *et al.*⁽⁸⁾ This shift may be explained by the lower kinetic energy of O^- ions in CO_2 .

REFERENCES

1. G. E. Keller, R. A. Beyer, and L. M. Colonna-Romano, *Phys. Rev. A* 8, 1446 (1973).
2. I. R. Gatland, L. M. Colonna-Romano, and G. E. Keller, *Phys. Rev. A* 12, 1885 (1975).
3. J. L. Pack and A. V. Phelps, *J. Chem. Phys.* 44, 1870 (1966).
4. H. W. Ellis, R. Y. Pai, I. R. Gatland, E. W. McDaniel, R. Wernlund, and M. J. Cohen, *J. Chem. Phys.* 64, 3935 (1976).
5. D. MacNair, *Rev. Sci. Instrum.* 38, 124 (1967).
6. G. L. Schulz, *Phys. Rev.* 128, 178 (1962). See also, E. W. McDaniel, *Collision Phenomena in Ionized Gases* (John Wiley & Sons, Inc. New York, 1964) p. 419.
7. J. Dutton, "A Survey of Electron Swarm Data," *J. Phys. Chem. Ref. Data*, 4, 681 (1975).
8. D. W. Goodson, R. J. Corbin, and L. Frommhold, *Phys. Rev. A* 9, 2049 (1974).
9. R. A. Beyer and J. A. Vanderhoff, *J. Chem. Phys.* 65, 2313 (1976).
10. J. T. Moseley, P. C. Cosby, R. A. Bennett, and J. R. Peterson, *J. Chem. Phys.* 65, 2512 (1976).
11. M. D. Kregel, M. R. Sullivan, L. M. Colonna-Romano, and G. E. Keller, NAPS Document #02183; order from ASIS/NAPS c/o Microfiche Publications, 305 E. 46 St., New York, N.Y. 10017. See also Ballistic Research Labs. Report No. 1617 (AD 907581).
12. J. Dutton, *op. cit.*, p. 720.
13. *Ibid.*, p. 605, 662-663.
14. G. H. Wannier, *Phys. Rev.* 83, 281 (1951); 87, 795 (1952). See also E. W. McDaniel and J. T. Moseley, *Phys. Rev. A* 3, 1040 (1971) or E. W. McDaniel and E. A. Mason, *The Mobility and Diffusion of Ions in Gases*, (John Wiley & Sons, Inc., New York, 1973) p. 314.
15. We are indebted to Dr. R. J. Corbin for this suggestion.
16. J. T. Moseley, P. C. Cosby, and J. R. Peterson, *J. Chem. Phys.* 64, 4228 (1976).

REFERENCES (CONTD)

17. R. N. Varney, Phys. Rev. 174, 165 (1958); J. Chem. Phys. 31, 1314 (1959).
18. M. Zemansky, Heat and Thermodynamics (McGraw Hill Book Co., Inc. New York, 4th ed. 1957) p. 433.

DISTRIBUTION LIST

<u>No. of Copies</u>	<u>Organization</u>	<u>No. of Copies</u>	<u>Organization</u>
12	Commander Defense Documentation Center ATTN: DDC-TCA Cameron Station Alexandria, VA 22314	1	Commander US Army Materiel Development and Readiness Command ATTN: DRCDMA-ST 5001 Eisenhower Avenue Alexandria, VA 22333
1	Director Institute for Defense Analyses ATTN: Dr. E. Bauer 400 Army-Navy Drive Arlington, VA 22202	1	Commander US Army Aviation Systems Command ATTN: DRSAV-E 12th and Spruce Streets St. Louis, MO 63166
2	Director Defense Advanced Research Projects Agency ATTN: STO, CPT J. Justice, Dr. S. Zakanyca 1400 Wilson Boulevard Arlington, VA 22209	1	Director US Army Air Mobility Research and Development Laboratory Ames Research Center Moffett Field, CA 94035
2	Director of Defense Research and Engineering ATTN: CAPT K. Ruggles Mr. D. Brockway Washington, DC 20305	1	Commander US Army Electronics Command ATTN: DRSEL-RD Fort Monmouth, NJ 07703
4	Director Defense Nuclear Agency ATTN: STAP (APTL) STRA (RAAE) Dr. C. Blank Dr. H. Fitz, Jr. DDST Washington, DC 20305	4	Commander/Director US Army Electronics Command Atmospheric Sciences Laboratory ATTN: Dr. E. H. Holt Mr. N. Beyers Mr. F. Horning Dr. F. E. Niles White Sands Missile Range, NM 88002
2	DASIAC/DOD Nuclear Information and Analysis Center General Electric Company-TEMPO ATTN: Mr. A. Feryok Mr. W. Knapp 816 State Street P.O. Drawer QQ Santa Barbara, CA 93102	1	Commander US Army Missile Research and Development Command ATTN: DRDMI-R Redstone Arsenal, AL 35809
		1.	Commander US Army Tank Automotive Development Command ATTN: DRETA-RWL Warren, MI 48090

DISTRIBUTION LIST

<u>No. of Copies</u>	<u>Organization</u>	<u>No. of Copies</u>	<u>Organization</u>
1	Commander US Army Mobility Equipment Research & Development Command ATTN: Tech Docu Cen, Bldg 315 DRSME-RZT Fort Belvoir, VA 22060	2	Commander US Army BMD System Command ATTN: SSC-HS, Mr. H. Porter SSC-TET, Mr. E. Carr P.O. Box 1500 Huntsville, AL 35807
1	Commander US Army Armament Command Rock Island, IL 61202	1	Director US Army Ballistic Missile Defense Technology Office ATTN: Mr. C. McLain 5001 Eisenhower Avenue Alexandria, VA 22333
2	Commander US Army Harry Diamond Laboratories ATTN: DRXDO-TI DRXDO-NP, Mr. F. Wimenitz 2800 Powder Mill Road Adelphi, MD 20783	1	HQDA (DAEN-RDM/Dr. F. de Percin) Washington, DC 20314
1	Director US Army TRADOC Systems Analysis Agency ATTN: ATAA-SA White Sands Missile Range NM 88002	3	Commanding Officer US Army Research & Standardization Group (Europe) ATTN: Dr. H. Lemons, Dr. G. R. Husk LTC J. Kennedy Box 15 FPO New York 09510
1	Commander US Army Nuclear Agency ATTN: Dr. J. Berberet Fort Bliss, TX 79916	1	Chief of Naval Research ATTN: Code 418, Dr. J. Dardis Department of the Navy Washington, DC 20360
3	Commander US Army Research Office ATTN: Dr. A. Dodd, Dr. D. Squire Dr. R. Lontz P.O. Box 12211 Research Triangle Park, NC 27709	1	Commander US Naval Surface Weapons Center ATTN: Dr. L. Rutland Silver Spring, MD 20910
2	Director US Army BMD Advanced Technology Center ATTN: Mr. M. Capps Mr. W. Davies P.O. Box 1500 Huntsville, AL 38507	1	Commander US Naval Electronics Laboratory ATTN: Mr. W. Moler San Diego, CA 92152

DISTRIBUTION LIST

<u>No. of Copies</u>	<u>Organization</u>	<u>No. of Copies</u>	<u>Organization</u>
4	Commander US Naval Research Laboratory ATTN: Dr. W. Ali Dr. D. Strobel Code 7700, Mr. J. Brown Code 2020, Tech Lib Washington, DC 20375	2	Sandia Laboratories ATTN: Dr. R. O. Woods Dr. F. Hudson P.O. Box 5800 Albuquerque, NM 87115
4	HQ USAF (AFNIN; AFRD; AFRDQ/ ARTAC/COL C. Anderson) Washington, DC 20330	4	Director National Aeronautics and Space Administration Goddard Space Flight Center ATTN: Dr. E. Hilsenrath Dr. V. Kunde Dr. A. Aikin Dr. R. Goldberg (Code 912) Greenbelt, MD 20771
9	AFGL (LKB, Dr. K. Champion, Dr. W. Swider Dr. J. Paulson Dr. T. Keneshea; LKD, Dr. R. Narcisi; OPI, Dr. J. Garing OPR, Dr. H. Gardiner Dr. Murphey Dr. Kennelly) Hanscom AFB, MA 01730	2	Director National Science Foundation ATTN: Dr. F. Eden Dr. G. Adams 1800 G Street, N.W. Washington, DC 20550
2	AFSC (DLCAW, LTC R. Linkous; SCS) Andrews AFB Washington DC 20334	2	General Electric Company Valley Forge Space Technology Center ATTN: Dr. M. Bortner Dr. T. Baurer P.O. Box 8555 Philadelphia, PA 19101
1	Director National Oceanic and Atmospheric Administration US Department of Commerce ATTN: Dr. E. Ferguson Boulder, CO 80302	2	Lockheed Palo Alto Research Laboratory ATTN: Dr. J. Reagan Mr. R. Sears 3251 Hanover Street Palo Alto, CA 94304
4	Director Los Alamos Scientific Laboratory ATTN: Dr. W. Maier (Gp J-10) Dr. J. Zinn (MS 664) Dr. W. Myers Dr. M. Peek P.O. Box 1663 Los Alamos, NM 87544	1	Mission Research Corporation ATTN: Dr. M. Scheibe 735 State Street P.O. Drawer 719 Santa Barbara, CA 93101

DISTRIBUTION LIST

<u>No. of Copies</u>	<u>Organization</u>	<u>No. of Copies</u>	<u>Organization</u>
1	Mitre Corporation ATTN: Tech Lib P.O. Box 208 Bedford, MA 01730	1	Systems, Science & Software ATTN: Dr. R. Englemore P.O. Box 1620 La Jolla, CA 92037
1	R&D Associates ATTN: Dr. F. Gilmore P.O. Box 9695 Marina Del Rey, CA 90291	1	Teledyne-Brown Engineering Company, Inc. SETAC ATTN: D. Lambert Research Park Huntsville, AL 35807
1	The Rand Corporation ATTN: Dr. C. Crain 1700 Main Street Santa Monica, CA 90406	1	TRW Systems Group ATTN: Tech Lib One Space Park Redondo Beach, CA 90278
2	Science Applications, Inc. ATTN: Mr. R. Lowen, Mr. D. Hamlin 1250 Prospect Plaza La Jolla, CA 92037	1	United Aircraft Research Laboratories ATTN: Dr. W. J. Wiegand, Jr. East Hartford, CT 06108
1	Science Applications, Inc./ Huntsville ATTN: Mr. R. Byrn 2109 West Clinton Avenue Suite 100 Huntsville, AL 35805	1	Visidyne, Inc. ATTN: Dr. H. Smith 19 Third Avenue, N.W. Industrial Park Burlington, MA 01803
1	Spectra Research Systems, Inc. ATTN: Mr. B. Kilday 2212 Dupont Drive Irvine, CA 92664	1	Columbia University ATTN: Dr. R. Zare 116th Street & Broadway New York, NY 10027
1	Stanford Research Institute ATTN: Dr. J. Peterson 333 Ravenswood Avenue Menlo Park, CA 94025	2	Georgia Institute of Technology School of Physics ATTN: Dr. I. Gatland Dr. E. McDaniel Atlanta, GA 30332
1	Systems Control, Inc. ATTN: Mr. R. Foerster 260 Sheridan Avenue Palo Alto, CA 94306		

DISTRIBUTION LIST

<u>No. of Copies</u>	<u>Organization</u>	<u>No. of Copies</u>	<u>Organization</u>
1	Pennsylvania State University Ionospheric Research Laboratory ATTN: Dr. L. Hale University Park, PA 16802	1	University of Illinois Department of Electrical Engineering ATTN: Dr. C. Sechrist, Jr. Urbana-Champaign Campus Urbana, IL 61801
1	State University of New York Department of Atmospheric Sciences ATTN: Dr. V. Mohnen Albany, NY 12203	1	University of Minnesota, Morris Division of Science and Mathematics ATTN: Dr. M. N. Hirsh Morris, MN 56267
1	University of Colorado CIRES ATTN: Dr. A. W. Castleman Boulder, CO 80302	2	University of Pittsburgh Cathedral of Learning ATTN: Dr. M. A. Biondi Dr. F. Kaufman 400 Bellefield Avenue Pittsburgh, PA 15213
2	University of Colorado Joint Institute for Laboratory Astrophysics ATTN: Dr. W. C. Lineberger Dr. A. V. Phelps Boulder, CO 80302	1	University of Texas at El Paso Physics Department ATTN: Ms. J. Collins El Paso, TX 79902
1	University of Delaware Department of Physics ATTN: Dr. S. B. Woo Newark, DE 19711	1	Utah State University Center for Research in Aeronomy ATTN: Dr. L. Megill Logan, UT 84321
2	University of Denver Denver Research Institute ATTN: Dr. R. Amme Dr. D. Murcray P.O. Box 10127 Denver, CO 80210	1	Wayne State University Department of Engineering ATTN: Dr. R. Kummeler Detroit, MI 48202
			<u>Aberdeen Proving Ground</u>
			Marine Corps LnO Dir, USAMSAA